Available online at www.sciencedirect.com

ScienceDirect

Energy Procedia 39 (2013) 408 – 414

Energy Procedia

Asian Nuclear Prospects 2012

(ANUP2012)

The Solubility of Rare Earth with Variable Valent and Electrochemical Behavior in LiCl–KCl–$AlCl_3$ Melts

YAN Yongde[a,b,*], LI Xing[b], ZHANG Milin[b], TANG Hao[b], HAN Wei[b], XUE Yun[a,b], and ZHANG Zhijian[a]

[a] *Key Discipline Laboratory of Nuclear Safety and Simulation Technology, Harbin Engineering University, , Harbin 150001, China*

[b] *Key Laboratory of Superlight Materials and Surface Technology, Ministry of Education,Harbin Engineering University, Harbin 150001, China*

Abstract

The solubility of RE_2O_3 (RE=Sm, Yb, and Eu) with variable valent in LiCl–KCl melts is extremely low. It is impossible to directly extract variable valent metals from RE_2O_3 using electrolysis in molten salts. After adding $AlCl_3$ to the melt system, the solubility measurements of RE_2O_3 in LiCl–KCl and LiCl–KCl–$AlCl_3$ melts indicate that $AlCl_3$ can effectively chloridize RE_2O_3. Take Yb_2O_3 as an example, the solubility of Yb_2O_3 in the LiCl–KCl–$AlCl_3$ melts increases first and decreases afterwards due to the rapid volatility of $AlCl_3$ with increase of temperature. The thermodynamic calculation of the reaction of Yb_2O_3 and $AlCl_3$ also indicates that the reaction would proceed forward at 753 K. Electrochemical behavior of RE_2O_3 on a molybdenum electrode in LiCl–KCl melts containing $AlCl_3$ also indicates that RE_2O_3 is effectively chloridized by $AlCl_3$, and then discharges in the form of RE(III) ions in the cathode. The underpotential deposition of RE on pre-deposited aluminum leads to the formation of Al-RE alloy. The extraction of RE with variable valent from RE oxide in LiCl–KCl melts is proven to be feasible.

Keywords: Pyrochemical reprocessing; Electroextraction; Lanthanides; Electrodeposition; Molten chlorides

* Corresponding author. Tel.: +86-451-82569890; fax: +86-451-82533026.
E-mail address: y5d2006@hrbeu.edu.cn..

doi:10.1016/j.egypro.2013.07.230

1. Introduction

Pyro-metallurgical reprocessing as a partitioning process which is expected to be a key technology to reduce the output and long-lived radiotoxicity of spent fuel and high-level waste (HLW) at the end of advanced fuel cycle [1]. In the pyro-metallurgical reprocessing, for example, the spent metal fuel is electrochemically dissolved into molten chlorides or fluorides as an anode. U, Pu and minor actinides, the most radiotoxic elements, are selectively gathered onto a solid cathode or recovered into a liquid metal, usually Fe, Cd, Bi, Ga or Al by electrorefining [2–6]. This process allows the selective extraction of actinides while lanthanides (Lns) remain in the salts.

After the selective extraction of the Ans, the rest Lns should be extracted from the melts for recycling the molten solvent. Special attention must be paid to the lanthanides (Lns) not only for its chemical similarity with respect to the actinides, that makes its mutual separation difficult, but also because of their neutronic poison effect, that could reduce the efficiency of the transmutation process [7]. Of these Lns, more attention should be paid to Lns with variable valents (Lns= Eu, Sm, and Yb) due to their special electrochemical properties. For example, it is impossible to prepare variable valent RE metals directly by electrolysis from molten salt, since the reduction potential of RE(II) to RE(0) is even more negative than the solvent in the chloride system.

Since the use of a reactive cathode allows the deposition potential of RE(II) ions moved to more positive direction by co-reduction with Al(III) ions. This so-called “depolarization effect” allows the theoretical extraction efficiency of these lanthanides to be enhanced up to 100% [8]. Reactive Al cathode is selected due to the strong interactions formed between the Ln and Al. Compared with a direct Al cathode, co-reduction of Ln with aluminium ions for the extraction of Ln shows some advantages [9]. To the best of my knowledge, the use of rare earth oxides as precursor for their extractions has not been reported.

2. Experimental

2.1. Purification of the melts and solubility measurement of RE_2O_3

A mixture of LiCl–KCl (1:1 wt.%, analytical grade) was first dried under vacuum for more than 72 h at 473 K to remove excess water, and then melted in an alumina crucible placed in a quartz cell located in an electric furnace. The temperature of the melts was measured with a nickel–chromium thermocouple sheathed with an alumina tube. Metal ion impurities in the melts were removed by pre-electrolysis at −2.10 V (vs. Ag^+/Ag) for 4 h. Aluminum and RE elements were introduced into the bath in the form of dehydrated $AlCl_3$ and RE_2O_3 powder. To determine the solubility of Yb_2O_3 in the LiCl-KCl melts at 753 K, the Yb_2O_3 powder was added into the LiCl-KCl melts and held for 3 h, and then the samples were taken from the clear supernatant fluid in the molten salt mixtures. After the clear supernatant fluid samples were solidified, each sample was dissolved in distilled water for analysis. The solution was diluted and analyzed using an inductively coupled plasma atomic emission spectrometer (ICP-AES, IRIS Intrepid II XSP, Thermo Elemental). The contents of K^+, Li^+, Al^{3+}, and Yb^{3+} measured by ICP were converted to the masses of KCl, LiCl, and Yb_2O_3, and then the solubilities of Yb_2O_3 in LiCl-KCl and LiCl–KCl–$AlCl_3$ melts were calculated.

2.2. Electrochemical apparatus and electrodes

All electrochemical measurements were performed using Im6eX electrochemical workstation (Zahner Co., Ltd.) with the THALES 3.08 software package. A silver wire (d =1 mm) dipped into a solution of

AgCl (1 wt.%) in LiCl–KCl melts contained in a Pyrex tube was used as the reference electrode. All potentials were referred to this Ag^+/Ag couple. A spectral pure graphite rod (d=6 mm) served as the counter electrode. The working electrodes were tungsten wires (d=1 mm, 99.99% purity), which were polished thoroughly using SiC paper, and then cleaned ultrasonically with ethanol prior to use. The active electrode surface area was determined after each experiment by measuring the immersion depth of the electrode in the molten salts.

2.3. Preparation and characterization of deposits

The samples of Al–Li–Eu alloys were prepared by galvanostatic electrolysis under different conditions at 953 K. After electrolysis, all samples were washed in hexane (99.8% purity) in an ultrasonic bath to remove salts and stored in the glove box for analysis. These deposits were analyzed by X-ray diffraction (XRD, X' Pert Pro; Philips Co., Ltd.) using Cu-Kα radiation at 40 kV and 40 mA. The specimens for microstructure morphology were mounted in thermosetting resins using a metallographic mounting press and then mechanically polished. Then, the microstructure and micro-zone chemical analysis were measured with scanning electron microscopy (SEM) and energy dispersive spectrometry (EDS, JSM-6480A; JEOL Co., Ltd.).

3. Results and discussion

3.1. The solubility measurements of Yb_2O_3 in LiCl–KCl and LiCl–KCl–$AlCl_3$ molten salts

Papatheodorou *et al*. [10] have reported that:

$$Sm_2O_3\,(s) + Al_2Cl_6\,(g,l) \rightarrow Al_2O_3\,(s) + 2SmCl_3\,(s) \qquad (1)$$

Therefore, Al_2Cl_6 can chloridize Sm_2O_3 into $SmCl_3$. We believe that the RE_2O_3 can also be effectively chloridized by $AlCl_3$ in the LiCl–KCl melts, and then discharges in the form of RE(III) ions in the cathode. In order to prove this assumption, the solubilities of RE_2O_3 in LiCl–KCl and LiCl–KCl–$AlCl_3$ melts were determined. To investigate the reaction between $AlCl_3$ and RE_2O_3, Yb_2O_3 is taken as an example. The solubility of Yb(III) in LiCl-KCl and LiCl-KCl-$AlCl_3$ molten salt was determined by ICP. Fig. 1 shows that the concentration of Yb(III) is very low in LiCl-KCl molten salt, and it almost has no relationship with temperature. Therefore, Yb_2O_3 has low solubility in LiCl-KCl melt. However, after adding $AlCl_3$(2 wt.%), the concentration of Yb(III) increases sharply. At first, its concentration increases along with the increase of temperature until to 750 K. Whereas as the temperature continues to increase, the solubility of Yb_2O_3 starts to decrease. This is due to the fact that $AlCl_3$ is volatile.

Fig.2 shows the relationship between the solubility of Yb_2O_3 and the amount of the addition of $AlCl_3$. The concentration of Yb(III) increase along with the increase of the concentration of $AlCl_3$. When all of the added Yb_2O_3 changed to Yb(III), the concentration of Yb(III) becomes constant. To further prove the chlorination of $AlCl_3$ to Yb_2O_3, some more experiments were carried out. We found Yb_2O_3 completely sediment down to bottom in water, which indicates Yb_2O_3 is insoluble in aqueous. However, when the Yb_2O_3 and $AlCl_3$ were mixed together and the mixture was held for a period of time at temperature of 573 K, the product can be dissolved in the water completely. The reaction of Yb_2O_3 chlorinated by $AlCl_3$ may be as the following reaction:

$$Yb_2O_3\,(s) + 2AlCl_3\,(l) \rightarrow Al_2O_3\,(s) + 2YbCl_3\,(s) \qquad (2)$$

From the thermodynamic data [11], Gibbs energy of this reaction at 753 K is calculated to be less than zero. The value of Gibbs energy means that the reaction (2) would proceed forward at our experimental temperature. This reaction is similar to the vapor process investigated by Papatheodorou *et al*. [10]. Hence based on the thermodynamics and the dynamics dates, $AlCl_3$ can chloridize Yb_2O_3 into Yb(III).

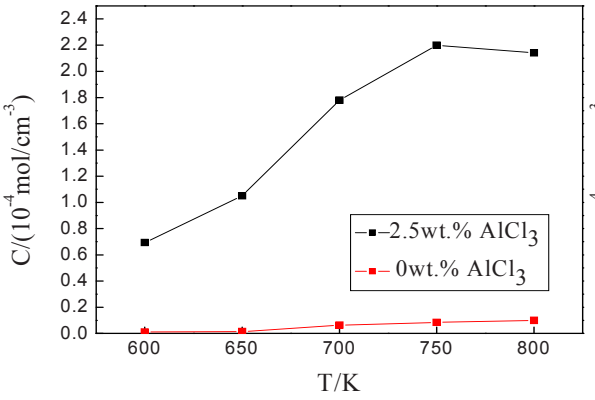

Fig. 1 The concentration of Yb(III) in LiCl-KCl and LiCl-KCl-$AlCl_3$(2 wt.%) molten salt at various temperature

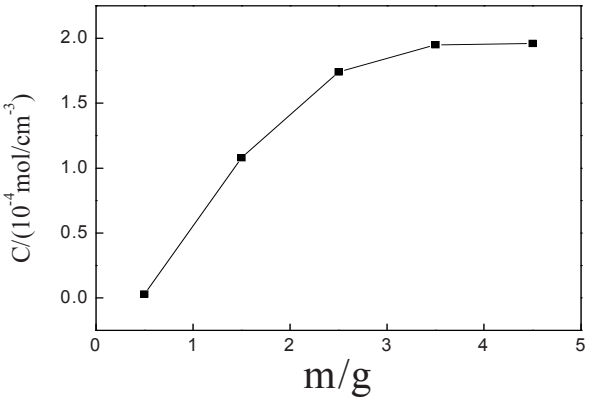

Fig. 2 The concentration variation of Yb(III) with the content of $AlCl_3$ in LiCl-KCl-$AlCl_3$ molten salt

3.2. Electrochemical behavior of RE_2O_3 in LiCl–KCl–$AlCl_3$ melts

In order to investigate the electrochemical property of RE_2O_3 in LiCl–KCl molten salt, the cyclic voltammograms at a W electrode obtained in LiCl–KCl system before and after the addition of RE_2O_3 (1 wt.%) was studied. The curve of blank LiCl–KCl almost coincides with the one of adding Yb_2O_3. After the addition of RE_2O_3, no obvious signal is observed, which indicates that no free RE(III) ions in the system. Fig. 3 shows the CVs obtained on molybdenum electrodes (S = 0.322cm^2) at various scan rates and cathodic limits with the addition of 2 wt. % $AlCl_3$ and 1wt. % Sm_2O_3, Yb_2O_3, and Eu_2O_3 in LiCl-KCl melts at 753 K, respectively. The peak currents increase with the increase of scan rate. From Fig. 3a, since the deposition of Al is close to the reduction of the Sm(III) to Sm(II), the reducation/oxidation peaks (E_1/E_1') prior to Al redox couple (A/A′) could be related to the redox reaction of Sm(III)/Sm(II) or the formation and oxidation of Al-Mo alloy, or their combination. In order to figure out who is responsible for the peaks E_1/E_1'. We carried out the CVs obtained on molybdenum electrodes at various scan rates in KCl-LiCl-$AlCl_3$-Yb_2O_3 melts (see Fig. 3b), due to a larger potential difference between deposition potential of Al and reduction one of the Yb(III) to Yb(II). The redox peaks (E_2/E_2') occurring at about -0.5 V correspond to the reduction/oxidation of Yb(III)/Yb(II). The shoulder F′ prior to Al oxidation peak is likely to be associated with the oxidation Al-Mo alloy deposited. To further investigate the formation of Al-Mo alloy, the CVs at various scan rates in KCl-LiCl-$AlCl_3$-Eu_2O_3 melts with a narrow potential window were performed (see Fig. 3c). One couple of redox current waves (F/F′) prior to Al redox peaks truly exists. Sometimes its cathodic current is easy to be hidden by a larger-scaled cathodic current of Al reduction and it is hard to be discovered. Oppositely, a CV with a wider potential window in KCl-LiCl-$AlCl_3$-Eu_2O_3 melts was conducted (Fig. 3d). The cathodic and anodic limits of the electrochemical window correspond to the reduction of Li^+ and the oxidation of chloride ions, respectively. The redox peaks (E_3/E_3') occurring at about 0 V correspond to the reduction/oxidation of Eu(III)/Eu(II). No formation or oxidation current of Al-Mo alloy is observed in the potential range of +1.0 to -1.5 V. We interpreted that as due to the small formation current of Al-Mo alloy.

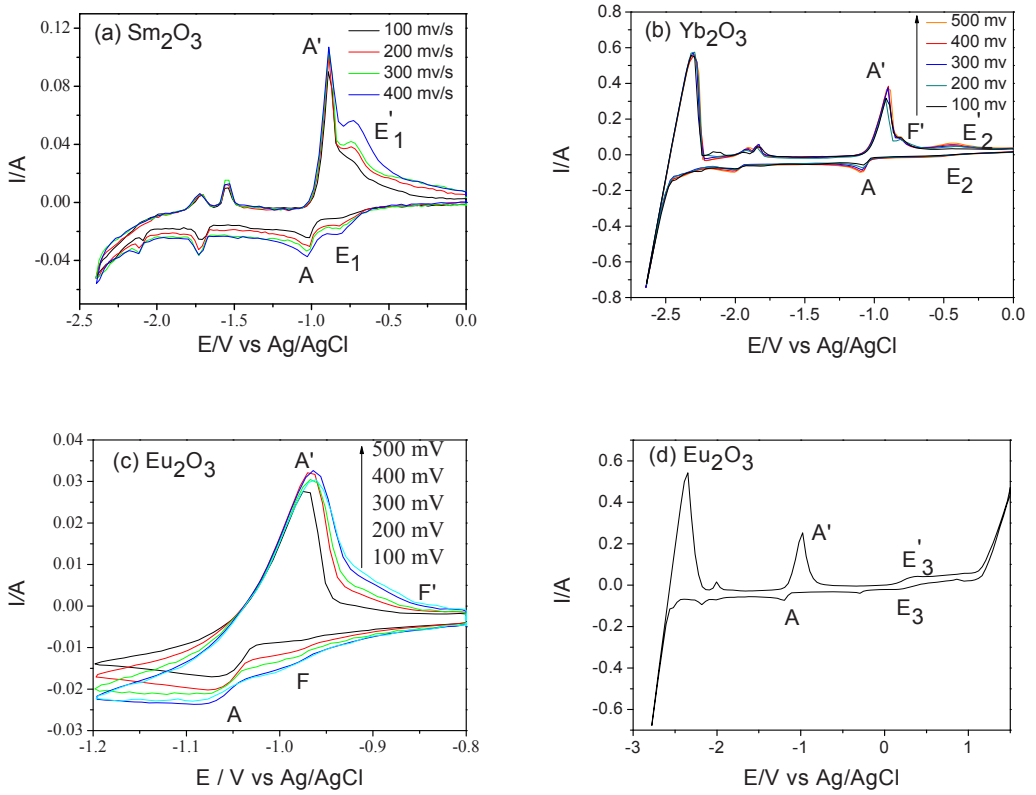

Fig. 3 CVs obtained on molybdenum electrodes ($S = 0.322cm^2$) at various scan rates and cathodic limits with the addition of 2 wt. % $AlCl_3$ and 1wt. % (a) Sm_2O_3 (b) Yb_2O_3 (c,d) Eu_2O_3 in LiCl-KCl melts at 753 K.

3.3. Galvanostatic electrolysis and characterization of the deposits

In the electrolytic experiments, we took Eu_2O_3 as raw material to extract Eu. The preparation of Al–Li–Eu alloys via galvanostatic electrolysis has been attempted with various electrolysis time in LiCl–KCl–Eu_2O_3(1 wt.%) –$AlCl_3$(14 wt.%) melts at 753 K. Fig. 4a–e shows the complicated XRD patterns of Al–Li–Eu alloy samples obtained by galvanostatic electrolysis from the LiCl–KCl–Eu_2O_3 –$AlCl_3$ melts at 2 A for different durations. As seen from the XRD patterns, the Al–Li–Eu alloys are composed of Al_2Li_3, AlLi, Al_2Eu, Al_4Eu and Al phases. With increasing electrolysis time, Al–Li alloy shows a phase transition from Al_2Li_3 to AlLi. Therefore, Al–Li–Eu alloys with different Li contents can be obtained by controlling the electrolysis time.

To examine the distribution of elements of Al and Eu in the Al–Li–Eu alloy, a mapping analysis of the elements was employed. Fig. 5 show a group of SEM and EDS mapping analysis of the Al–Li–Eu alloy by co-dreduction from LiCl–KCl–Eu_2O_3 (1 wt. %) melts containing 14 wt. % $AlCl_3$. From the SEM image, many flower-like and needle-like precipitates were observed on the surface of Al–Li–Eu alloy. The mapping analysis of element shows that the element of Eu mainly distributes on the flower-like and needle-like precipitate and does not distribute homogeneously in the Al–Li–Eu alloy.

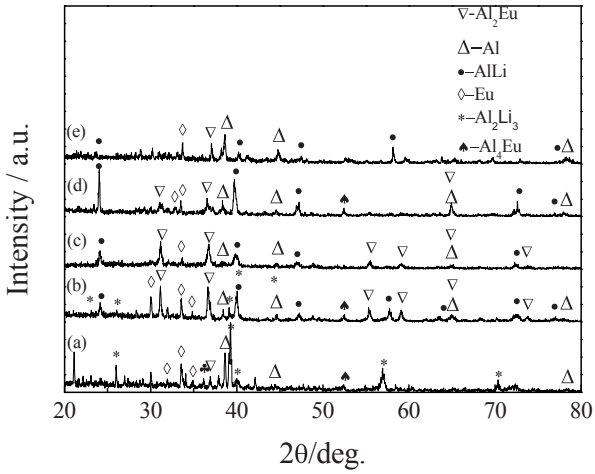

Fig. 4. XRD patterns of deposits obtained by galvanostatic electrolysis on W electrodes (S = 0.636 cm^2) in the LiCl–KCl–Eu_2O_3(1 wt.%) –$AlCl_3$(14 wt.%) melts with at 2 A for different electrolysis durations (a) 0.5; (b) 1; (c) 1.5; (d) 2; (e) 3 h.

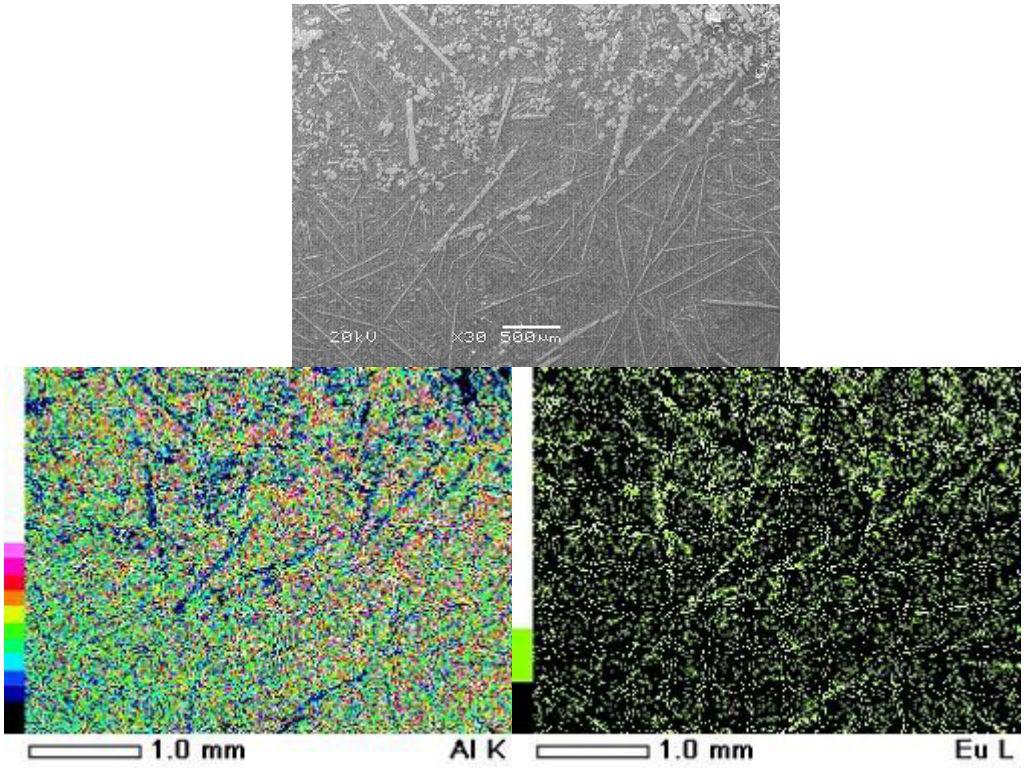

Fig. 5. SEM and EDS mapping analysis of the Al–Li–Eu alloy by co-reduction from LiCl–KCl–$AlCl_3$(14 wt.%) – Eu_2O_3(1 wt.%) melt.

4. Conclusions

Electrochemical behavior of RE_2O_3 with variable valent on a molybdenum electrode in LiCl–KCl melts containing $AlCl_3$ at 753 K was investigated by cyclic voltammograms. The results of cyclic voltammetry indicates that the underpotential deposition of RE on pre-deposited aluminum leads to the formation of Al-RE (RE = Sm, Yb, and Eu) alloy. The solubility measurements of Yb_2O_3 in LiCl–KCl and LiCl–KCl–$AlCl_3$ melts indicate that $AlCl_3$ can effectively chloridize Yb_2O_3. The structure, morphology, and energy dispersion analysis of deposit obtained by galvanostatic electrolysis were analyzed, and the formation of Al-Li-Eu alloys was confirmed. This new technique overcomes the limitation of low RE_2O_3 solubility in molten salts, and opens up unprecedented opportunities for the extraction of RE with variable valent from RE oxide in molten chlorides.

Acknowledgements

The work was financially supported by High Technology Research and Development Program of China (No. 2011AA03A409), the National Natural Science Foundation of China (21103033 and 21101040), the Fundamental Research funds for the Central Universities (HEUCF101002), the Heilongjiang Postdoctoral Fund (LBH-Z10196 and LBH-Z10207) and China Postdoctoral Science Foundation (20100480974). The authors are particularly grateful to Dr. Tom Mann for kindly discussing various parts of the manuscript.

References

[1] L.H. Baetslé, T. Wakabayashi, S. Sakurai, Status and assessment report on actinide and fission product partitioning and transmutation, OECD/NEA, Working group on P&T (1998).

[2] M. Kurata, Y. Sakamura, T. Hijikata, K. Kinoshita, J. Nucl. Mater., 227 (1995)110–121.

[3] M. Iizuka, K. Uozomi, T. Inoue, T. Iwai, O. Shirai, Y. Arai, J. Nucl. Mater., 299 (2001) 32–42

[4] O. Shirai, M. Iizuka, T. Iwai, Y. Arai, Anal. Sci., 17 (2001) 51–57.

[5] D. Lambertin, S. Ched'homme, G. Bourges, S. Sanchez, G.S. Picard, J. Nucl. Mater., 341 (2005) 131–140

[6] L. Rault, M. Heusch, M. Allibert, F. Lemort, X. Deschanel, R. Boen, Nucl. Technol., 139 (2002) 167–174.

[7] Y. Castrillejo, P. Fernández, M.R. Bermejo, E. Barrado, and A.M. Martínez, *Electrochim. Acta*, **54** 6212–6222 (2009).

[8] C. Nourry, L. Massot, P. Chamelot, P. Taxil, J. Appl. Electrochem. 39 (2009) 2359.

[9] P. Taxil, L. Massot, C. Nourry, M. Gibilaro, P. Chamelot, and L. Cassayre, J. Fluor. Chem. 130 (2009) 94–101.

[10] G.N. Papatheodorou, G.H. Kucera, Inorg. Chem. 18 (1979) 385.

[11] I. Barin, Thermochemical Data of Pure Substances (3rd Edition), Wiley-VCH Verlag GmbH, Weinheim, Germany, 1995.